Effect of steel fiber on fracture characteristics and ductility of self-compacting concrete: experimental and theoretical investigation

Hadi Heydarpour[a], Siroos Gholampour[a], Habib Akbarzadeh Bengar[b*]

a. *Department of Civil Engineering, Qaemshahr Branch, Islamic Azad University, Qaemshahr, Iran*

b. *Department of Civil Engineering, University of Mazandaran, Babolsar, Iran*

[*] Corresponding Author: E-mail address: h.akbarzadeh@umz.ac.ir, Tel: +98 9111165785

Hadi Heydarpour is PhD candidate in civil engineering department at Islamic Azad University (Qaemshahr Branch), Iran. His research interests include the mechanical and durability properties of fiber reinforced concrete and self-compacting concrete and behavior of fiber reinforced concrete member in flexure and compression, fracture properties of steel fiber reinforced concrete and self-compacting concrete.

Siroos Gholampour is an Assistant Professor in the department of civil engineering at Islamic Azad University (Qaemshahr Branch). He received his Master degree from University of Tabriz, Iran in 1991 and his PhD degree from Islamic Azad University (Science and Research Branch), Iran in 2006, respectively. His research interests include the seismic behavior and design of steel frame and steel shear wall system, optimization of steel structures.

Habib Akbarzadeh Bengar is an Associate Professor of department of civil engineering at the University of Mazandaran. He received his Master and PhD degrees from University of Kerman, Iran in 2004 and 2010, respectively. His research interests include the mechanical and durability properties of geo-polymer concretes and 3D printed concrete, behavior of fiber reinforced concrete member in flexure and compression, strengthening of reinforced concrete structures with FRP, seismic behavior and design of reinforced concrete frame and shear wall system and behavior of concrete structures under fire.

Abstract. Understanding the performance of self-compacting concrete (SCC) during fracture is of particular interest when designing SCC members and helps to better predict the performance of SCC structures. Moreover, adding steel fibers in SCC can change the cracking pattern and fracture performance. Hence, 75 notched SCC beams containing steel fibers at volume percentages of 0.15, 0.3, 0.45, and 0.6% were made in this work and tested under the three-point bending load to investigate their brittleness and fracture behavior. To this end, work of fracture method (WFM) and size effect method (SEM) were used to analyze the fracture parameters. The results showed that increasing the steel fiber content from 0.15 to 0.6% increased fracture energy values obtained from WFM and SEM by 9.8 and 2.5 times, respectively, compared to SCC without fibers. Also, at a steel fiber content of 0.6%, the characteristic length of concrete (l_{ch}) in WFM, and the fracture process zone (C_f) and fracture toughness (K_{IC}) in SEM were 5.4, 3.3 and 1.7 times, respectively, those of SCC without fibers. The results of l_{ch} in WFM and C_f in SEM showed that the fibrous SCC samples were more ductile.

Keywords: Fracture parameters; Steel fiber; Brittleness number; Fracture toughness; Self-compacting concrete (SCC).

1. Introduction

1.1. Self-compacting concrete containing fibers

Recently, the development of concrete technology has made it possible to produce concretes with higher performance and strength than those of conventional concrete. Among these, self-compacting concrete (SCC) has been considered by many researchers due to its flowability and workability properties. Self-compacting concrete (SCC) is a high-flowability concrete that becomes compacted under its own weight with no need for mechanical vibration and completely fills the mold; this way, the produced mixture is homogenous without segregation [1-3]. Moreover, by employing SCC, there are many options for the structural design and architecture [4]. On the other hand, the significant place of concrete in the construction industry along with its weak tensile response have led to the interest of researchers in using steel fibers in concrete mixtures [5]. As reported in the literature, the incorporation of fiber in concrete mix not only enhances the mechanical features such as compressive, tensile, and flexural strengths, as well as elastic modulus, but also enables the production of workable concrete with more energy absorption and less cracking [6]. Furthermore, fibers reduce the brittle response of concrete and control the growth and propagation of cracks through the mechanism of fiber-bridging [7, 8]. Parameters contributing to this enhancement in the performance of fibrous SCC generally has a strong dependence on the material, shape, content, tensile capacity, and bridging action of the fibers [9, 10]. Many studies have been done by researchers on the use of fibers in SCC. Among them, Majain *et al.* [11] in a study evaluated the compressive strength of SCC containing steel fibers. Results demonstrated that incorporating steel fibers in SCC, in addition to lowering the performance of concrete, can increase the compressive strength of concrete and make the distribution of cracks more uniform. Moreover, multiple studies have addressed the energy-absorption capacity of fiber-reinforced concrete and concluded that fibers hinder the propagation of cracks in concrete and improve the energy-absorption capacity. Alberti *et al.* [12] reported that adding fibers to ordinary concrete and SCC increased energy-absorption capacity, particularly in the post-peak stage. Turk *et al.* [6] also investigated the impact of steel fiber on the mechanical features of SCC. The obtained results showed that the performance of SCC decreased with raising the content of steel fibers, while compressive strength, flexural strength, and ductility increased.

1.2. Fracture mechanic of self -compacting concrete

The fracture mechanics of concrete is one of the most basic pieces of information needed to design and evaluate the safety and durability of structures, especially in big structural systems like tunnels, nuclear containment facilities, and dams [13, 14]. Many factors, including cavities in the cement paste, difference between the moduli of the aggregates and the matrix, and poor interface of aggregates and the cement paste give rise to microcracks and their diffusion inside concrete; hence, given the existence of numerous microcracks in concrete, its mechanical performance is affected [7]. Nevertheless, one of the most essential factors directly related to the fracture characteristics of concrete is the interfacial transition zone (ITZ), in which the highest number of microcracks occur, and indeed, this zone can be considered as the most vulnerable area in the concrete [15]. The use of fibers in SCC can change the cracking behavior and fracture parameters of this concrete [15]. Also, many new materials are used to improve the cracking resistance of building materials in addition to fibers [16-18]. Cement additives in SCC improve the microstructure of ITZ between aggregates and cement paste and in turn enhance the cracking behavior of concrete [19-21].

Many studies have investigated the fracture characteristics of SCC. Raisi *et al.* [22] found that adding rice husk ash to SCC lowered the fracture energy and negatively affected the concrete ductility; in other words, the concrete became more brittle. In another study, Ghasemi *et al.* [23] investigated the fracture characteristics of fiber-reinforced SCC and reported that increasing the volume fraction of fibers improved the fracture energy and made the concrete more ductile. The WFM and SEM were utilized to calculate the fracture energy, and G_F/G_f ratio was obtained as 9.66 for the SCC reinforced with steel fibers. In addition, Rajeshwari and Sivakumar [24] concluded that increasing the diameter and content of coarse particles in SCC improved the fracture energy. As reported by Çelik and Bingöl [25], adding different fiber types including polypropylene, glass, and basalt to SCC samples improved their fracture energy while slightly changing the compressive capacity.

1.3. Research significance and novelty

Considering that the actual behavior of structures cannot be obtained by analysis and design methods that are based on stress and strength criteria, the fracture mechanics theories can be used to investigate the actual behavior of structures. Although design codes have not been able to incorporate fracture mechanics principles to this day, the importance of this approach and attempts to obtain the actual structural behavior through its principles have not diminished. On the other hand, many researchers have tried to present proper models for the prediction of the fracture parameters of concrete based on the semi-brittle behavior of concrete. The parameters usually change with variations in different ambient and internal factors such as the mix design ingredients. Therefore, in this study, based on the obtained mechanical properties and test variables, multivariate models have been proposed to predict the fracture parameters of SCC containing steel fibers, and the results of these models were compared with the experimental results of this study and those by others.

Hence, in this research, 75 notched beams were made to evaluate the effect of using steel fibers at volume percentages of 0, 0.15, 0.3, 0.45, and 0.6% on the fracture characteristics and brittleness of SCC under a three-point bending test. For the purpose of analysis and interpretation of fracture parameters, two methods, namely the work of fracture method (WFM) and the size effect method (SEM), were used.

1.4. The limitations and assumptions of the research.

Using steel fibers negatively affects the rheological properties of fresh self-compacting concrete and lowers its workability. In this research, to reach the plastic viscosity of interest for the concrete mixes, steel fibers with volume fractions of up to 0.6% were used since using higher fiber contents leads to the fresh concrete properties that are outside the recommended ranges of EFNARC.

In this study, the type and quality of materials in different mix designs were assumed identical. In addition, the distribution of fibers in the SCC volume was considered to be uniform.

2. Determination of fracture parameters

2.1. Work of fracture method

Among different methods put forward for determining fracture parameters of concrete, the work of fracture method (WFM), proposed by RILEM FMC-50 [26], is extensively applied in research works. Since WFM uses the three-point flexural test on beams, the maximum particle diameter and the standard table are used to specify the dimensions of these beams [27]. Hence, to determine fracture energy (G_F) in WFM, the following equation is used,

$$G_F = \frac{W_F}{b(d - a_0)} \quad (1)$$

In which, G_F and W_F give fracture energy obtained from WFM and total fracture energy (area enclosed by the load-displacement diagram), respectively, both in $N.mm$. Moreover, b and d respectively give the beam width and height, while a_0 gives the depth of notch (mm). The above-mentioned model proposed by Hillerberg *et al.* [28] indicates that parameter G_F alone cannot serve as a proper measure to represent concrete ductility and brittleness. Hence, the characteristic length of concrete was presented as Eq. (2):

$$l_{ch} = \frac{EG_F}{f_t^{\,2}} \quad (2)$$

In which l_{ch} is the characteristic length (mm), E is the elastic modulus (MPa), and f_t is the splitting tensile strength (MPa), respectively. Parameter l_{ch} serves as an index of the concrete ductility, and thus, lower values of l_{ch} show that the concrete is less ductile and crack resistant [29-31].

2.2. Size effect method

RILEM FMT-89 [32] proposes the size effect method (SEM) as an applicable method. This method does not depend on the size, shape, and type of sample. To determine fracture parameters in SEM, samples with identical geometries and distinct dimensions are subjected to the three-point flexural experiment. To determine the nominal capacity of concrete samples with identical geometries, the size effect law can be employed according to Eq. (3),

$$\sigma_N = \frac{B}{(1+\beta)^{0.5}}, \ \beta = \frac{d}{d_0} \tag{3}$$

In which β gives the brittleness number of Bažant and Kazemi [33], indicating the mode of fracture. Also, d_0 and β are empirical parameters related to the geometry and material features of the structure. For samples with similar geometries in two dimensions, the value of σ_N is determined by substituting the experimental values in Eq. (4),

$$\sigma_N = \mathrm{C}_n \frac{P_u}{bd} \tag{4}$$

In which C_n is a constant coefficient, and P_u is the peak load (N). Moreover, d and b are the depth and width of the beam (mm), respectively. By applying the linear regression on the peak loads of samples with identical geometries and distinct dimensions and utilizing Eq. (3), parameters d_0 and B can be obtained.

$$Y = AX + C \tag{5}$$

In the above, $Y = (\frac{1}{\sigma_N})^2$, $X = d$, $d_0 = \frac{C}{A}$, and $B = \frac{1}{\sqrt{C}}$. Moreover, the slope of regression line is represented by A, while the distance of y-intercept from this line is represented by C.

Furthermore, to obtain fracture energy, G_f, and effective length of fracture process zone (FPZ), C_f, the LEFM (linear elastic fracture mechanics) measure is used.

$$G_f = \frac{g(\alpha_0)}{AE} \tag{6}$$

$$C_f = \frac{g(\alpha_0)}{g'(\alpha_0)} \times \frac{C}{A} \tag{7}$$

In the above, $g(\alpha_0)$ represents energy release rate (dimensionless function of the structural geometry), and $g'(\alpha_0)$ is the first derivative of $g(\alpha_0)$ with respect to $\alpha_0 = \frac{a_0}{d}$. $g(\alpha_0)$ and $g'(\alpha_0)$ are obtained using the LEFM criterion [32]. The remaining parameters of fracture in SEM are the fracture toughness (K_{IC}) and effective crack mouth opening displacement (δ_C) which can be calculated by Eqs. (8) and (9),

$$K_{IC} = \sqrt{EG_f} \tag{8}$$

$$\delta_C = \frac{8K_{IC}}{E} \times \sqrt{\frac{C_f}{2\pi}} \tag{9}$$

In which K_{IC} and δ_C are expressed in MPa.mm$^{0.5}$ and mm, respectively.

3. Testing step

3.1. Ingredients and mixture ratios

Here, five SCC mixes with a water to cement ratio of 0.44 and different volume fractions of fibers were designed. Crushed sand with a modulus of 2.7, density of 2.63 in the saturated surface dry (SSD) state, and water-absorption level of 1.7% and crushed gravel with a water-absorption level of 0.9%, density of 2.68, and maximum particle diameter of 9.5 mm were used as the fine and coarse aggregates, respectively. Portland cement type II supplied from Neka Cement Factory, Mazandaran, Iran, with a density of 3.15, was added to the SCC mixtures. Ultra-fine limestone powder was also used to achieve the desired plastic viscosity for concrete mixes. In this study, double-hooked steel fibers with a length of 35 mm and an aspect ratio of 43.75 were used at four different volume fractions of 0.15, 0.3, 0.45, and 0.6%. Fiber shape and properties are presented in Figure 1 and Table 1, respectively. In addition, in all the concrete mixtures, a superplasticizer (SP) based on polycarboxylate ether with a solid content of 40% and a specific gravity of 1.1 was used as a weight percentage of cement.

The SCC concrete mixing plan for 1 m^3 is given in Table 2. To achieve a uniform and homogeneous mixture, all the designs were mixed in a laboratory mixer for 6 minutes. Since the concrete type was SCC, the features of fresh concrete were considered according to the recommendations of EFNARC [34], and the results are illustrated in Table 3. The names of the mixtures are given in Table 2, in which SCC-ST0 represents the plain (fiber-free) SCC, while SCC-ST0.15, SCC-ST0.3, SCC-ST0.45, and SCC-ST0.6 indicate SCCs containing 0.15, 0.3, 0.45, and 0.6% steel fibers, respectively.

3.2. Samples and test setup

Three notched beam samples with a fixed length of 840 mm and cross-section dimensions of 100 × 100 mm were manufactured from each mixture to measure the fracture properties in WFM. To create the vertical notch, a 3-mm-thick wood plate was placed at mid-length of the beams in the tension side. The ratio of the notch depth to the beam depth (a_0/d) was 0.5 for the samples (shown in Figure 2).

Beside WFM samples, another group of notched flexural samples were prepared based on the maximum aggregate size in concrete to obtain the fracture parameters in SEM based on RILEM FMT-89 [32]. In this method, the beams had the same width of 38.1 mm and variable depths of 38.1, 76.2, 154.4, and 304.8 mm. In addition, the length to depth ratio was constant and equal to 2.67, and also, the span length to the depth ratio was equal to 2.5. In this method, the depth of the initial notch is equal to 0.2 of beam depth ($a_0 = 0.2d$). Hence, given the presence of four distinct heights in the beams, each beam had a different notch depth depending on the height. In this method, three notched samples were made for each depth. Photos of the manufactured SEM samples of various dimensions can be seen in Figure 3a, with their geometry shown in Figure 3b.

In addition, in accordance with BS EN 12390 [35], for each laboratory group, three $100 \times 100 \times 100$ mm cubic samples were made to evaluate the compressive strength (f_c), and six 150×300 mm cylinder samples were manufactured, of which three samples were made for the elastic modulus test (E) and the other three for the tensile test (f_t) in accordance with ASTM C469 [36] and ASTM C496 [37], respectively. The samples dimensions in this research for different experiments are presented in Table 4. All concrete samples were removed from the molds after 24 hours and cured for 28 days in accordance with ASTM C192 [38]. Here, all the notched beam samples were subjected to the three-point flexural experiment by a 250-kN universal testing machine (UTM), and the displacement was controlled during the loading. The loading rates of the notched beams were constant and equal to 0.4 mm/min in WFM and 0.1 mm/min in SEM [39, 40].

4. Analysis of results

4.1. Mechanical characteristics

Table 5 summarizes the results of mechanical tests on the SCC samples containing steel fibers. Moreover, Figure 4 shows the values of mechanical features normalized relative to those of SCC-ST0. This figure shows that adding steel fiber to SCC improves the compressive strength. By increasing the volume fraction of steel fibers from 0 to 0.6%, the compressive strength of the SCC increased by 14%. The improvement in the compressive capacity of concrete containing fibers can be attributed to the ability of fiber to inhibit the crack propagation, lower stress concentration at crack tip, change direction of cracks, and delay growth rate of cracks by bridging them [41, 42]. In addition, Table 5 and Figure 4 demonstrate that raising volume fraction of steel fibers to 0.6% increases tensile capacity and elastic modulus by 39.8 and 8.2%, respectively. It was found that because of the existence of fiber in the brittle cement matrix, crack width in the SCC samples was smaller, which led to higher flexural and tensile strengths. In addition, fibers improved the stiffness of the concrete by providing the cohesion and adhesion, as well as controlling the width of the cracks and reducing the growth rate of the cracks [43].

4.2. Analyzing fracture using WFM

4.2.1. Load-displacement curves from WFM

Figure 5 gives the load-displacement graph of the beam samples incorporating steel fibers obtained from WFM. For samples containing fibers, the curves reached a maximum load and then experienced a sudden drop in the load-carrying capacity. The SCC samples had high strength values; thus, the curve of SCC samples, even in the presence of fibers, dropped after the maximum load, similar to the reports of other researchers [23, 40]. Moreover, raising the steel fiber content improves the deformation at the midspan and decreases the mean slope in the post-peak area, indicating that the concrete shows greater ductility. In addition, increasing the volume fraction of fibers in the beam samples leads to an increase in the area under the load-displacement curve, which indicates their higher energy absorption. It can be observed in Table 5 and Figure 5 that the amount of steel fiber directly affects fracture energy of concrete: raising the content of fiber considerably improves the fracture energy. This increase occurs since raising the percentage of steel fiber results in the passage of more fibers through the fracture surface; as a result, for cracks to propagate, more energy is needed.

4.2.2. Fracture energy (G_F)

The average fracture energy values of SCC samples with separate contents of steel fiber according to WFM are presented in Figure 6 and Table 5. As can be seen, the volume fraction of steel fibers considerably affects G_F, such that with raising the content of steel fiber up to 0.6%, the amount of fracture energy of the SCC reached 9.79 times that of plain concrete. By forming bridges between two crack sides, the fibers delay the growth rate of the crack and inhibit its expansion, and thus, the energy absorption increases [44].

According to CEB-FIP [45] and other studies [29, 33], it is possible to express G_F based on compressive capacity. Here, values given in Table 5 were used to express the relationship of G_F, f_c, and the amount of fibers as Eq. (10).

$$\frac{G_{F,v_f}}{G_{F,0}} = 15.4 V_f^{\,1.1} + 0.96\,\alpha_f^{\,0.2} \qquad R^2 = 0.99 \tag{10}$$

In the above equation, $\alpha_f = \frac{f_{c,v_f}}{f_{c,0}}$, in which f_{c,V_f} and $f_{c,0}$ give compressive strength values of the sample containing steel fibers and the sample without fibers, respectively. G_{F,v_f} and $G_{F,0}$ are fracture energy values according to WFM for the sample containing fibers and the sample without fibers, respectively. V_f is the amount of steel fiber in the concrete. According to Table 5 and Eq. (10), increasing the compressive strength and fiber content in SCC samples causes an increase in G_F.

The failure energy predictions were compared with the laboratory data of other studies in the literature on concrete containing steel fibers (Beigi *et al.* [39], Ghasemi *et al.* [44], and Mousavi *et al.* [15]) in Figure 7a. Also, Figure 7b shows the ratio of laboratory values to predicted fracture energy values against the steel fiber content. Figure 7a indicates that the proposed concrete fracture energy model agrees well with the present results and the laboratory results of other studies. Moreover, according to Figure 7b, the experimental failure energy values of Ghasemi *et al.* [44] and Mousavi *et al.* [15] for different fiber contents are in proper agreement with the values of proposed model; however, for the sample containing 0.2% fibers, the developed model and laboratory data of Mousavi *et al.* [15] have maximum difference.

4.2.3. The characteristic length (l_{ch})

The parameter l_{ch} is known as an indicator of concrete ductility in WFM (Eq. (2)). Figure 8 shows the effect of volume fraction of fibers on l_{ch}. The lowest value of l_{ch} was 166.1 mm in the sample without fibers, indicating the brittle behavior of the SCC in this case. Moreover, the sample containing 0.6% fibers showed the maximum value of this parameter, indicating the most ductile behavior. Figure 8 indicates that as the steel fiber content increases, the value of l_{ch} in SCC increases. In this regard, raising the fiber content from 0.15 to 0.6% increased the value of this parameter from 462.2 to 900.8 mm. Higher values of l_{ch} in samples containing greater fiber contents show their better crack resistance [46].

According to the data in Table 5, a relation for predicting parameter l_{ch} based on the variables of compressive strength of concrete (α_f or f_c) and volume fraction of fibers (V_f) is presented in Eq. (11),

$$\frac{l_{ch,v_f}}{l_{ch,0}} = 6.2V_f^{\,0.54} + \alpha_f^{\,-0.58} \qquad R^2 = 0.98 \tag{11}$$

Where $l_{ch,0}$ gives the characteristic length of concrete in the control sample, and l_{ch,v_f} is the characteristic length of concrete for samples containing fibers.

Figure 9a compares prediction values for the characteristic length of fiber-reinforced SCC in WFM with the laboratory results of Beigi *et al.* [39] and Mousavi *et al.* [15]. Moreover, Figure 9b shows the ratio of laboratory values to predicted values of characteristic length vs. the volume fraction of fibers. Figure 9 show that the developed characteristic length model of concrete correlates well with laboratory data of Beygi *et al.* [39], Mousavi *et al.* [15], and the results of the present study.

4.3. Assessment of fracture parameters using SEM

One of the size-independent methods for the calculation of the fracture parameters is size effect method (SEM). In this method, three important fracture parameters including G_f, C_f, and K_{IC} are obtained. When calculating the peak load according to RILEM FMT-89 [32], it is necessary to consider the sample weight. Hence, Eq. (12) is used to correct the peak load as follows,

$$P_n^0 = P_n + \frac{2S_n - L_n}{2S_n} \times g \times m_n \tag{12}$$

In which P_n^0 and P_n give the modified peak load and the peak load recorded by the test devices, respectively; m_n, S_n, and L_n are the mass, span length, and length of sample, respectively; g is gravity acceleration; n gives number of tested samples (between 1 and total number of samples).

Table 6 gives modified peak loads for beams incorporating steel fibers. Based on the modified peak load values, linear regression was conducted and fracture parameters of the SCC samples in SEM were determined by Eq. (5), as can be seen in Figure 10. This figure shows that raising the content of steel fiber in the SCC reduces the slope and increases the width of the source determined using linear regression. This demonstrates a considerable rise in the fracture toughness and energy of the SCC. Furthermore, RILEM FMT-89 [32] recommends that to enhance the linear analysis accuracy, variation coefficients of the slope of regression line (W_A) and the width of origin (W_C), and the relative width of the scatter bar (m) should not exceed 1, 0.2, and 0.2, respectively. Table 7 shows that all the samples stay below the recommended limits, indicating that the analysis is properly accurate.

4.3.1. Initial fracture energy (G_f)

Table 7 gives the values of initial failure energy, G_f. In addition, Figure 11 gives the variation of G_f with the content of steel fiber in the SCC samples. The fiber-free sample had the lowest value of G_f among all the samples: about 48 N / m. On the other hand, raising the content of fiber in the SCC samples significantly increased the initial fracture energy. In this regard, raising the content of fiber from 0.15 to 0.6% increased parameter G_f from 56.8 to 121.8 N /m. The value of G_f in sample SCC-ST0.6 was about 2.54 times that of the reference sample (SCC-ST0). The fibers delay the onset and propagation of the microcracks by bridging the microcracks, thus improving the load-bearing capacity of the beam and the initial failure energy [40].

The initial fracture energy and compressive strength increased with increasing the fiber volume fraction in the SCC. As reported by others such as Kazemi *et al.* [40], Kumar and Reddy [47], and Mousavi *et al.* [15], raising the content of fibers in concrete leads to higher compressive strength and initial fracture energy values.

By using the data in Table 7, a relation for G_f is presented based on the compressive strength of concrete (f_c or α_f) and volume fraction of fibers (V_f) as Eq. (13),

$$\frac{G_{f,v_f}}{G_{f,0}} = 3.77V_f^{\,1.34} + 0.99\alpha_f^{\,-3.4} \qquad R^2 = 0.99 \tag{13}$$

Where $G_{f,0}$ and G_{f,v_f} are fracture energy values based on SEM in the control and fiber-reinforced samples, respectively.

In Figure 12, predictions for the fracture energy of SCCs containing steel fibers in SEM are compared against the laboratory data of the current study and those in the literature (Kazemi *et al.* [40], Kumar and Reddy [47], and Mousavi *et al.* [15]). In addition, Figure 12b gives the ratio of laboratory to prediction results of fracture energy in SEM against the content of steel fibers. Figure 12a shows that the developed model for the concrete fracture energy and laboratory data of the current study and the literature correlate well. Also, Figure 12b demonstrates that the experimental fracture energy values reported by Kazemi *et al.* [40], Kumar and Reddy [47], and Mousavi *et al.* [15] in terms of the volume percentages of fibers are in good agreement with the corresponding values of the proposed model. However, in concrete containing 0.4% fibers, the largest difference between the proposed model and the experimental results of Kazemi *et al.* [40] and Mousavi *et al.* [15] is observed.

4.3.2. Effective length of fracture process zone (C_f)

Table 7 and Figure 13 show the variation of C_f with the volume fraction of fibers for the SCC samples. It is observed that adding steel fibers, even at small contents, considerably affects the brittle behavior of concrete in this method. From Table 7 and Figure 13, the value of C_f for the SCCs increases with raining the content of steel fiber. By adding up to 0.6% steel fibers to SCC, parameter C_f increased from 21.2 to 69.1 mm, indicating ductile response of the SCC containing steel fiber. Moreover, according to Table 7 and Figure 13, the SCC sample incorporating 0.6% steel fibers had a C_f value 3.3 times that of the SCC without fibers. Further, Figure 13 demonstrates that the characteristic length, l_{ch}, in WFM and the effective length of FPZ, C_f, in SEM have almost the same trend against the content of fiber.

Figure 14 shows fracture properties against the steel fiber content for the SCCs. As can be observed, increasing the volume fraction of steel fibers in the SCC increases the values of f_c, C_f and G_f. The high percentages of fibers in concrete not only improved its brittle behavior and reduced the stress concentration around the microcracks but also maximized the fractal dimension and made the concrete more ductile [40, 48]. The concrete fracture is often caused by the separation of the aggregate from the mortar, in which the first cracks occur at a point where the aggregate binds to the mortar, and as these cracks grow, larger cracks appear. Therefore, adding fibers prevents the spread of cracks and delays their growth.

4.3.3. Fracture toughness (K_{IC})

Fracture toughness (K_{IC}) values of the SCC samples reinforced with steel fibers can be seen in Table 7 and Figure 15. Parameter K_{IC} in the fiber-free SCC was around 40.4 MPa.mm$^{0.5}$. However, as the content of steel fiber in SCC increased, the fracture toughness saw a significant increase. In this regard, adding 0.6% steel fibers by concrete volume led to a 1.7 times increase in K_{IC}. In samples incorporating fibers, by adding 0.15, 0.3, 0.45, and 0.6% steel fibers, K_{IC} increased by 9.4, 32.2, 43.8, and 65.8%, respectively, compared to that of the reference sample (without fibers). Further, based on the results, with a small rise in the amount of steel fiber, fracture toughness improved, indicating a higher resistance of concrete with a higher fiber content against the unstable crack development [15]. The reason for this increase is that the fibers in the vicinity of the cement paste prevent the growth and expansion of microcracks and improve the brittle behavior of concrete, thereby increasing the fracture toughness of the concrete.

In other words, the bridging action of fibers at crack tips increased the fracture toughness of the concrete. In this regard, such that as the number of cracks increases, the initiation of crack propagation requires more energy. This is attributed to a greater role of fibers in the crack tip region, and fibers in the cracked region also resist against crack propagation. As the volume fraction of fibers increases, the number of microcracks in the concrete matrix increased, and when microcracks reach the tip of the initial crack, the initial crack deviates. This in turn leads to higher energy absorption in this region and increases the fracture toughness of concrete [40, 44].

According to the data in Table 7, a relation for predicting the fracture toughness parameter based on the variables of compressive strength of concrete (f_c or α_f) and volume fraction of fibers (V_f) is presented as Eq. (14).

$$\frac{K_{IC,v_f}}{K_{IC,0}} = 2.1V_f^{\ 1.25} + 0.99\alpha_f^{\ -3.94} \qquad R^2 = 0.99 \tag{14}$$

A comparison between the fracture toughness predictions and the laboratory results of the present work and works of Kazemi *et al.* [40], Noaman *et al.* [49], and Mousavi *et al.* [15] is provided in in Figure 16a. Furthermore, Figure 16b shows the ratio of laboratory values to predicted fracture toughness in terms of the fiber volume fraction. As can be seen in Figure 16a, the proposed model for the fracture toughness of concrete correlates well with the laboratory results. However, Figure 16b shows that at high volume fractions of the fibers, there is a relatively considerable difference between the proposed model and the laboratory results of Noaman *et al.* [49] and Mousavi *et al.* [15].

4.3.4. The Brittleness number (β)

Brittleness number (β) is a parameter of particular interest for estimating the fracture pattern. This parameter, which is independent of the sample geometry, is determined by Eq. (3), based on data provided in Table 7. As reported by Bazant and Kazemi [33], β governs the fracture manner of a structural member and also specifies criteria for its design. It is also reported that for $\beta < 0.1$, members have a ductile behavior, and analysis is performed according to the strength criterion. Once $0.1 \leq \beta \leq 10$, the nonlinear fracture mechanics governs the structural behavior. At last, for $\beta > 10$, the analysis is conduced based on LEFM criteria. According to Figure 17, β changes with the depth of the beam for the fiber-reinforced SCC samples. All the values in this figure correspond to the standard range for nonlinear fracture mechanics. Further, as the size of the sample increases compared with the length of FPZ, the design criteria approach the LEFM standard. Nevertheless, according to Table 7 and Figure 17, by raising the content of fiber, the performance of SCC approach the strength criterion. Further, SCC samples became considerably less brittle as the content of steel fibers increases.

4.4. Failure energy ratio obtained by WFM and SEM

As reported by Bazant and Kazemi [33], fracture energies determined based on WFM and SEM, G_F and G_f, respectively, which are both concrete properties, are related to one another. Note that G_F is always larger than G_f. For the analysis of concrete structures with high susceptibility to fracture, it is recommended to obtain G_F by means of G_f since direct determination is accompanied by high uncertainty, on one hand, and the scattering of fracture energy determined in SEM is smaller and its accuracy is greater in comparison with the fracture energy determined in WFM as a result of considering the structural size and shape, one the other hand. Therefore, determining the ratio of G_F/G_f is very important. For the present study, the values of G_F/G_f for the SCC samples with and without fibers are presented in Figure 18. The G_F/G_f ratio for the SCC without fibers was about 2.6. On the other hand, this ratio for the SCC containing steel fibers was on average 8.87 with a coefficient of variation of 19%. Beygi *et al.* [14, 39] estimated the ratio of G_F/G_f for fiber-free SCC as 2.92-2.7 with a coefficient of variation of 12.5%. Ghasemi *et al.* [44] reported that the value of G_F/G_f for SCC containing different contents of fibers was on average 8.89 with a coefficient of variation of 34%.

5. Conclusions

This study used 75 notched beams under three-point bending test to investigate the effect of adding steel fibers at volume percentages of 0.15, 0.3, 0.45, and 0.6% on fracture properties and ductility of SCC samples. To this end, the analysis and assessment of the fracture parameters were conducted using the work of fracture method (WFM) and size effect method (SEM). The main results of the present work are as follows.

- The mechanical features of SCC samples, namely compressive and tensile strengths and elastic modulus, increased by 14, 40, and 8%, respectively, when the content of steel fiber increased to 0.6%.
- The values of total fracture energy (G_F) obtained in WFM and initial fracture energy (G_f) obtained in SEM increased by 10 and 2.5 times with the increase in the volume fraction of steel fibers from 0.15 to 0.6%, respectively, compared to the SCC without fibers. In addition, in SCC containing steel fibers, fracture energies increased with increasing compressive strength. The G_F/G_f ratio increased from 2.6 for the SCC without steel fibers to about 8.87 for the SCC containing steel fibers.
- The load-displacement curves of the notched WFM beam samples show that raising the steel fiber content increases the deformation at mid-span and decreases the average slope in the post-peak part of the curve, which indicates the higher ductility behavior of concrete. In addition, by increasing the volume fraction of steel fibers from 0.15% to 0.6%, the value of l_{ch} increased from 462 to 901 mm. Therefore, a higher value of l_{ch} in samples with a larger content of fibers suggests their superior crack resistance.
- Raising the content of steel fibers to 0.6% in the SCC samples increased the fracture toughness, K_{IC}, from 40 to 67 MPa.mm$^{0.5}$ and the length of FPZ, C_f, from 21 to 69 mm. As fiber content reached 0.6% in the SCC, C_f and K_{IC} in SEM reached 3.3 and 1.7 times, respectively, those of the reference (fiber-free) sample. This shows an improved ductility of SCC with raising the fiber content.
- With increasing the dimensions of the sample compared to the length of FPZ, the design criterion became closer to the LEFM criterion. Also, based on SEM, by raising the steel fiber content, the performance of the SCC samples became closer to the strength criterion. Furthermore, SCC samples became considerably less brittle by raising the content of steel fibers.
- The values obtained for the mechanical features and test variables were employed to propose multivariate prediction models for the fracture behavior of SCC containing

steel fibers. The prediction results were compared with laboratory data of the current study and the literature, and a good correlation was observed.

Conflict of Interest

None

Nomenclature and Notation

SCC	Self-compacting concrete
SEM	Size effect method
WFM	Work of fracture method
a_0	Depth of notch (mm)
b	Beam width (mm)
C_f	Effective length of fracture process zone (mm)
C_n	Constant coefficient
d	Beam height (mm)
E	Modulus of elasticity (GPa)
f_c	Compressive strength (MPa)
f_t	Splitting tensile strength (MPa)
G_F	Total fracture energy (N/m)
G_f	Initial fracture energy (N/m)
g	Gravity acceleration (N/kg)
K_{IC}	Fracture toughness (MPa.mm$^{0.5}$)
l_{ch}	Characteristic length of concrete (mm)
L_n	Length of sample (mm)
m_n	Mass of sample (kg)
P_u	Ultimate peak load (N)
P_n^0	Modified peak load (N)
S_n	Span length of sample (mm)
V_f	Volume fraction of fiber

W_F The total amount of work of fracture in the test (N.mm)

β Brittleness number

δ_C Effective crack mouth opening displacement (mm)

σ_N Nominal strength (MPa)

References

1. Okamura. H. “Self-compacting high-performance concrete”, *Concrete international,* **19**(7), pp. 50-54 (1997).
2. Okamura, H. and Ozawa, K. “Self-compacting high performance concrete”, *Structural engineering international,* **6**(4), pp.269-270 (1996).
3. Hasan-Ghasemi, A., Nematzadeh, M. and Fallahnejad, H. “Post-fire residual fracture characteristics and brittleness of self-compacting concrete containing waste PET flakes: Experimental and theoretical investigation”, *Engineering Fracture Mechanics,* **261**, p.108263 (2022).
4. Jagadesh, P., de Prado-Gil, J., Silva-Monteiro, N. and Martínez-García, R. “Assessing the compressive strength of self-compacting concrete with recycled aggregates from mix ratio using machine learning approach”, *Journal of Materials Research and Technology*, **24**, pp.1483-1498 (2023).
5. Savinykh, A.S., Garkushin, G.V., Kanel, G.I. and Razorenov, S.V. “Compressive and tensile strength of steel fibrous reinforced concrete under explosive loading”, *International Journal of Fracture,* **215**, pp.129-138 (2019).
6. Turk, K., Bassurucu, M. and Bitkin, R.E. “Workability, strength and flexural toughness properties of hybrid steel fiber reinforced SCC with high-volume fiber”, *Construction and Building Materials*, **266**, p.120944 (2021).
7. Jafari, A., Preti, M., Beheshti, M. and Dugnani, R. “Self-centering walls strengthening by high-performance concrete: a feasibility study” *Materials and Structures*, **54**(3), p.117 (2021).
8. Alrawashdeh, A. and Eren, O. “Mechanical and physical characterisation of steel fibre reinforced self-compacting concrete: Different aspect ratios and volume fractions of fibres”, *Results in Engineering*, **13**, p.100335 (2022).

9. Tarifa, M., Poveda, E., Cunha, V.M. and Barros, J.A. "Effect of the displacement rate and inclination angle in steel fiber pullout tests", *International Journal of Fracture*, **223**(1-2), pp.109-122 (2020).
10. Arafa, M.H., Alqedra, M.A. and Almassri, H.G. "Effect of forta-ferro fibers on fresh and mechanical properties of ultra high performance self compacting concrete", *Int. J. Eng. Tech. Res*, **1**(7), pp.43-47 (2013).
11. Majain, N., Rahman, A.B.A., Mohamed, R.N. and Adnan, A. "Effect of steel fibers on self-compacting concrete slump flow and compressive strength", In *IOP Conference Series: Materials Science and Engineering* (Vol. 513, No. 1, p. 012007), IOP Publishing (2019).
12. Alberti, M.G., Enfedaque, A. and Gálvez, J.C. "Comparison between polyolefin fibre reinforced vibrated conventional concrete and self-compacting concrete", *Construction and Building Materials*, **85**, pp.182-194 (2015).
13. Bazant, Z.P. and Planas, J. "*Fracture and size effect in concrete and other quasibrittle materials*", Routledge (2019).
14. Beygi, M.H., Kazemi, M.T., Nikbin, I.M. and Amiri, J.V. "The effect of aging on the fracture characteristics and ductility of self-compacting concrete", *Materials & Design*, **55**, pp.937-948 (2014).
15. Mousavi, S.M., Ranjbar, M.M. and Madandoust, R. "Combined effects of steel fibers and water to cementitious materials ratio on the fracture behavior and brittleness of high strength concrete", *Engineering Fracture Mechanics*, **216**, p.106517 (2019).
16. Zhang, P., Han, S., Golewski, G.L. and Wang, X. "Nanoparticle-reinforced building materials with applications in civil engineering", *Advances in Mechanical Engineering*, **12**(10), p.1687814020965438 (2020).
17. Golewski, G.L. and Szostak, B. "Strength and microstructure of composites with cement matrixes modified by fly ash and active seeds of CSH phase", *Structural Engineering and Mechanics, An Int'l Journal*, **82**(4), pp.543-556 (2022).
18. Golewski, G.L. "An extensive investigations on fracture parameters of concretes based on quaternary binders (QBC) by means of the DIC technique", *Construction and Building Materials*, **351**, p.128823 (2022).
19. Golewski, G.L. "Comparative measurements of fracture toughgness combined with visual analysis of cracks propagation using the DIC technique of concretes based on cement matrix with a highly diversified composition", *Theoretical and Applied Fracture Mechanics*, **121**, p.103553 (2022).

20. Golewski, G.L. “Fracture performance of cementitious composites based on quaternary blended cements”, *Materials*, **15**(17), p.6023 (2022).

21. Golewski, G.L. “Combined effect of coal fly ash (CFA) and nanosilica (nS) on the strength parameters and microstructural properties of eco-friendly concrete”, *Energies*, **16**(1), p.452 (2022).

22. Raisi, E.M., Amiri, J.V. and Davoodi, M.R. “Influence of rice husk ash on the fracture characteristics and brittleness of self-compacting concrete”, *Engineering Fracture Mechanics*, **199**, pp.595-608 (2018).

23. Ghasemi, M., Ghasemi, M.R. and Mousavi, S.R. “Studying the fracture parameters and size effect of steel fiber-reinforced self-compacting concrete”, *Construction and Building Materials*, **201**, pp.447-460 (2019).

24. Rajeshwari, B.R. and Sivakumar, M.V.N. “Influence of coarse aggregate properties on specific fracture energy of steel fiber reinforced self-compacting concrete”, *Advances in Concrete Construction*, **9**(2), p.173 (2020).

25. Çelik, Z. and Bingöl, A.F. “Fracture properties and impact resistance of self-compacting fiber reinforced concrete (SCFRC)”, *Materials and Structures*, **53**, pp.1-16 (2020).

26. RILEM, D.R. “Determination of the fracture energy of mortar and concrete by means of three-point bend tests on notched beams”, Materials and structures **18**(106), pp. 285-290 (1985).

27. Akbari, M., Tahamtan, M.H.N., Fallah-Valukolaee, S., Herozi, M.R.Z. and Shirvani, M.A. “Investigating fracture characteristics and ductility of lightweight concrete containing crumb rubber by means of WFM and SEM methods”, *Theoretical and Applied Fracture Mechanics*, **117**, p.103148 (2022).

28. Hillerborg, A., Modéer, M. and Petersson, P.E. “Analysis of crack formation and crack growth in concrete by means of fracture mechanics and finite elements”, *Cement and concrete research*, **6**(6), pp.773-781 (1976).

9. Fallahnejad, H., Davoodi, M.R. and Nikbin, I.M. “The influence of aging on the fracture characteristics of recycled aggregate concrete through three methods”, *Structural Concrete*, **22**, pp.E74-E93 (2021).

30. Elices, M., Guinea, G.V. and Planas, J. “On the measurement of concrete fracture energy using three-point bend tests”, *Materials and structures*, **30**, pp.375-376 (1997).

31. RILEM TC 187-SOC. “Final Report of RILEM Technical Committee TC 187-SOC: Experimental determination of the stress crack opening curve for concrete in tension”, RILEM publications (2007).

32. Shah, S.P. “Size-effect method for determining fracture energy and process zone sizeof concrete”, *Materials and Structures,* **23**(6), pp. 461-465 (1990).

33. Bažant, Z.P. and Kazemi, M.T. “Determination of fracture energy, process zone length and brittleness number from size effect, with application to rock and concrete”, *International Journal of fracture,* **44**, pp.111-131 (1990).

34. EFNARC, S. “guidelines for self-compacting concrete”, English ed, European federation for specialist construction chemicals & concrete systems (2005).

35. B. En, “Method of determination of compressive strength of concrete cubes”, *Testing hardened concrete,* BS EN 12390 (2000).

36. ASTM C469. “Standard test method for static modulus of elasticity and Poisson’s ratio of concrete in compression”, *Annual book of ASTM standards* (2022).

37. ASTM C496. “Standard Test Method for Splitting Tensile Strength of Cylindrical Concrete Specimens”, *Annual book of ASTM standards* (2017).

38. ASTM C192. “Standard Practice for Making and Curing Concrete Test Specimens in the Laboratory”, *Annual book of ASTM standards* (2016).

39. Beygi, M.H., Kazemi, M.T., Nikbin, I.M. and Amiri, J.V. “The effect of water to cement ratio on fracture parameters and brittleness of self-compacting concrete”, *Materials & Design*, **50**, pp.267-276 (2013).

40. Kazemi, M.T., Golsorkhtabar, H., Beygi, M.H.A. and Gholamitabar, M. “Fracture properties of steel fiber reinforced high strength concrete using work of fracture and size effect methods”, *Construction and Building Materials*, **142**, pp.482-489 (2017).

41. Afroughsabet, V. and Ozbakkaloglu, T. “Mechanical and durability properties of high-strength concrete containing steel and polypropylene fibers”, *Construction and building materials,* **94**, pp.73-82 (2015).

42. Yan, H., Sun, W. and Chen, H. “The effect of silica fume and steel fiber on the dynamic mechanical performance of high-strength concrete”, *Cement and Concrete Research*, **29**(3), pp.423-426 (1999).

43. Akturk, B., Akca, A.H. and Kizilkanat, A.B. “Fracture response of fiber-reinforced sodium carbonate activated slag mortars”, *Construction and Building Materials,* **241**, p.118128 (2020).

44. Ghasemi, M., Ghasemi, M.R. and Mousavi, S.R. “Investigating the effects of maximum aggregate size on self-compacting steel fiber reinforced concrete fracture parameters”, *Construction and Building Materials*, **162**, pp.674-682 (2018).
45. C.-F.M. Code, First Draft, Committee Euro-International du Beton, Bulletin d’information 195 (1990) 196.
46. Şahin, Y. and Köksal, F. “The influences of matrix and steel fibre tensile strengths on the fracture energy of high-strength concrete”, *Construction and Building Materials,* **25**(4), pp.1801-1806 (2011).
47. Kumar, D.R. and Reddy, M.M. “August. Effect of fiber and aggregate size on fracture parameters of high strength concrete”, In *IOP Conference Series: Materials Science and Engineering* (Vol. 225, No. 1, p. 012288), IOP Publishing (2017).
48. Xie, C., Cao, M., Khan, M., Yin, H. and Guan, J. “Review on different testing methods and factors affecting fracture properties of fiber reinforced cementitious composites”, *Construction and Building Materials*, **273**, p.121766 (2021).
49. Noaman, A.T., Bakar, B.A., Akil, H.M. and Alani, A.H. “Fracture characteristics of plain and steel fibre reinforced rubberized concrete”, *Construction and Building Materials*, **152**, pp.414-423 (2017).

Figure 1. Steel fibers used in this research

Figure 2. Work of fracture sample

Figure 3. (a) SEM samples for three-point bending test; (b) geometry of beam samples according to SEM

Figure 4. Normalized f_c , f_t and E vs. steel fiber content

Figure 5. Load-displacement curves of SCC beams containing steel fibers.

Figure 6. Variation on the fracture energy of SCC with content of steel fibers using WFM

Figure 7. (a) Results of developed fracture energy model compared with laboratory data of other researchers and the present study; (b) the ratio of laboratory values to the predicted values of fracture energy versus volume fraction of fibers

Figure 8. Characteristic length values versus steel fiber content in SCC samples

Figure 9. (a) The results of developed characteristic length model of SCC compared with laboratory data of other researchers and present study; (b) the ratio of laboratory values to the predicted values of the characteristic length of SCC

Figure 10. Fracture parameters of SCC samples incorporating steel fibers in SEM obtained using linear regression

Figure 11. Initial fracture energy values against volume fraction of steel fibers

Figure 12. (a) The proposed initial failure energy model compared with the laboratory results of other researchers and the present study; (b) the ratio of laboratory values to the predicted values of failure energy versus volumetric fraction of steel fibers

Figure 13. Variation of C_f with volume fraction of steel fibers for SCC samples

Figure 14. Concrete fracture parameters against volume fraction of fibers in SCC samples

Figure 15. Fracture toughness for SCC samples against volumetric fraction of steel fibers

Figure 16. (a) Results of developed fracture toughness model compared with laboratory data of present and other research works; (b) the ratio of laboratory values to predicted values versus the volume fraction of steel fibers

Figure 17. Variation of brittleness number (β) with the beam depth for SCC containing fibers

Figure 18. Total-to-initial fracture energy ratio for SCC incorporating different steel fiber contents

Figure 1. Steel fibers used in this research

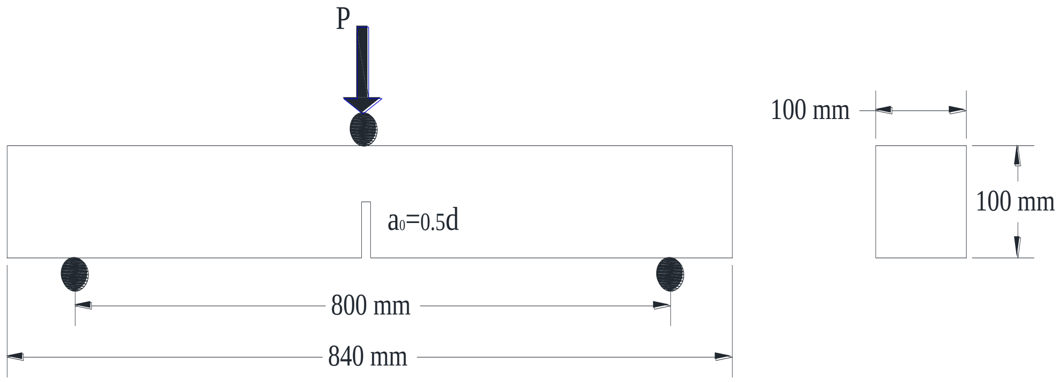

Figure 2. Work of fracture sample

(a)

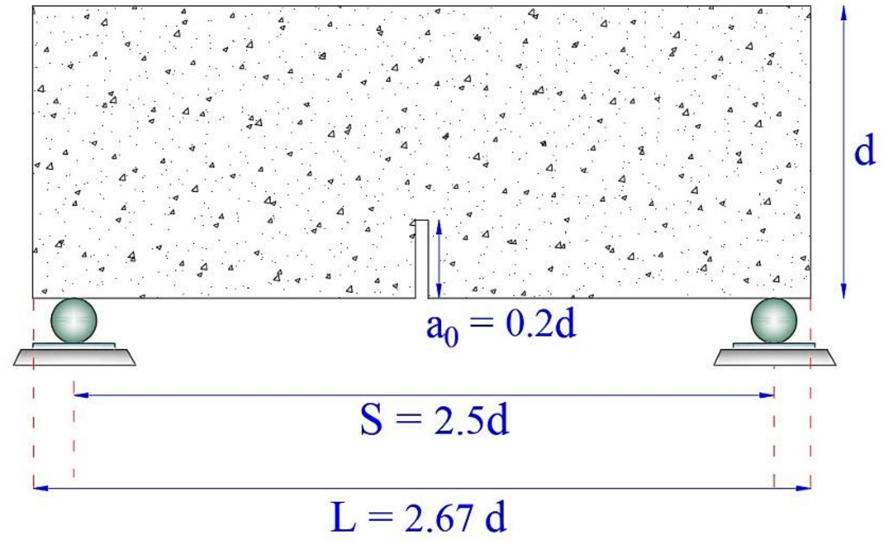

(b)

Figure 3. (a) SEM samples for three-point bending test; (b) geometry of beam samples according to SEM

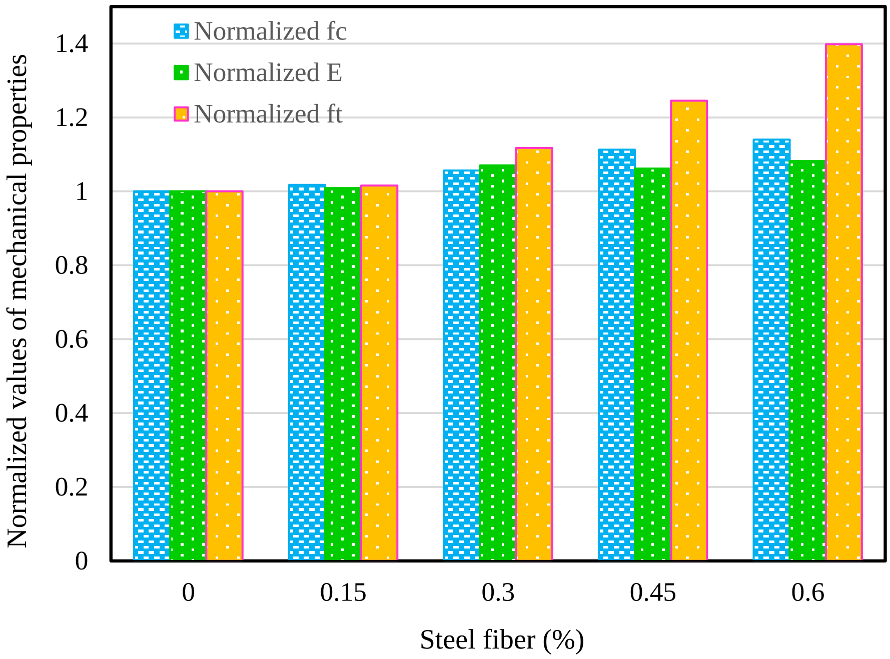

Figure 4. Normalized f_c, f_t and E vs. steel fiber content

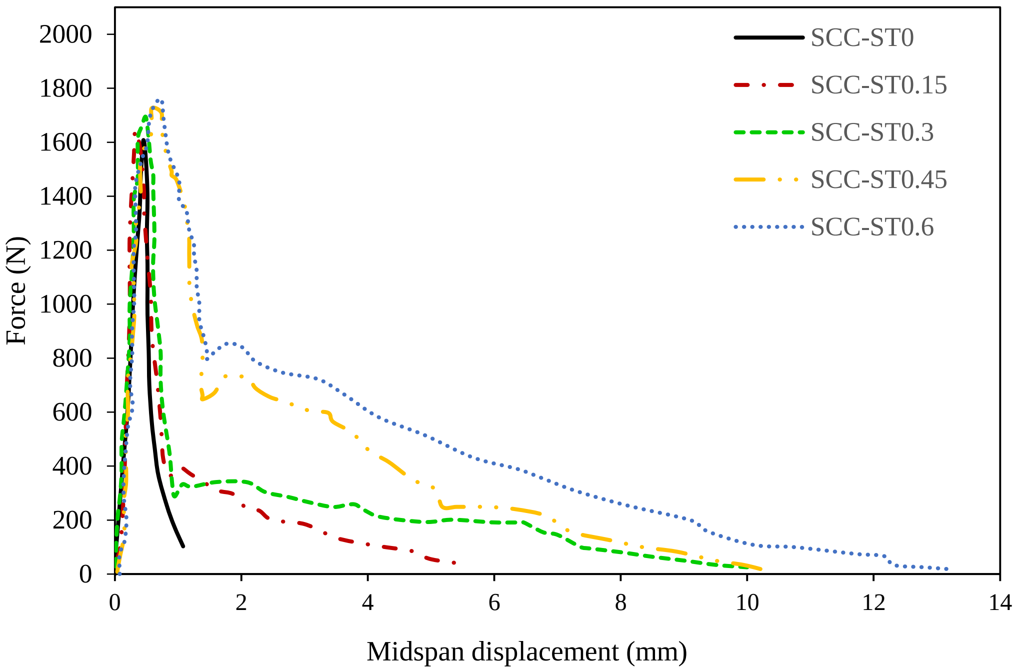

Figure 5. Load-displacement curves of SCC beams containing steel fibers.

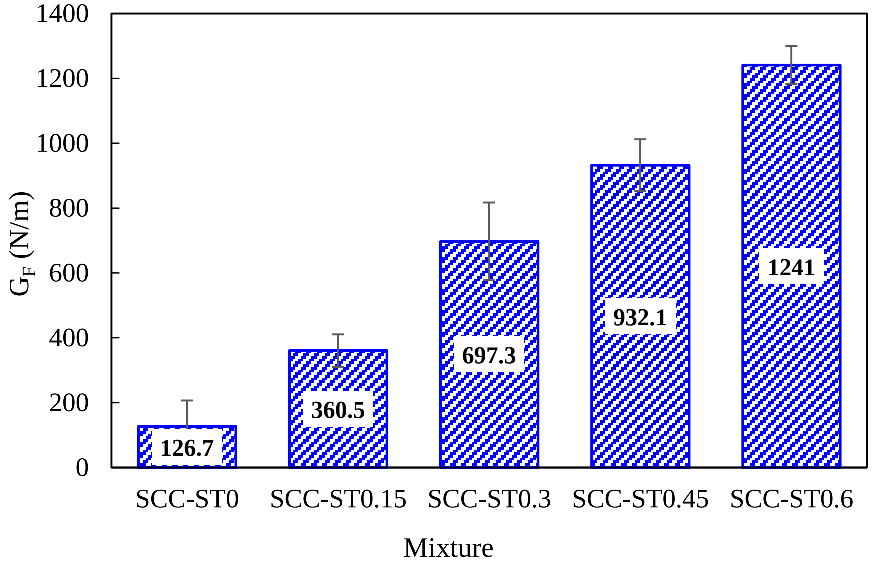

Figure 6. Variation on the fracture energy of SCC with content of steel fibers using WFM

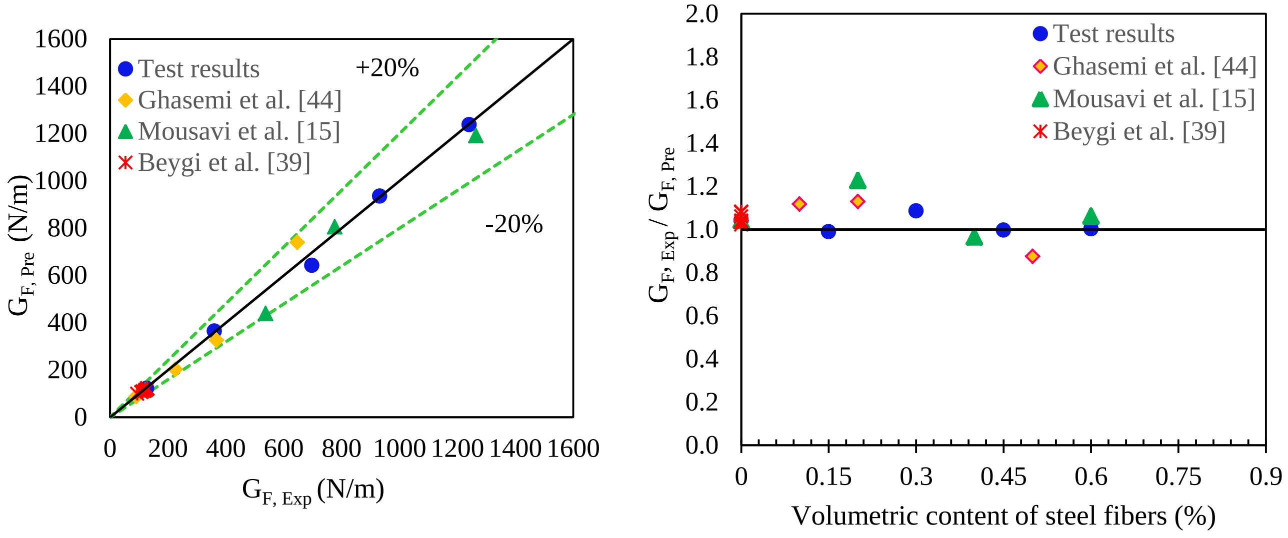

(a) **(b)**

Figure 7. (a) Results of developed fracture energy model compared with laboratory data of other researchers and the present study; (b) the ratio of laboratory values to the predicted values of fracture energy versus volume fraction of fibers

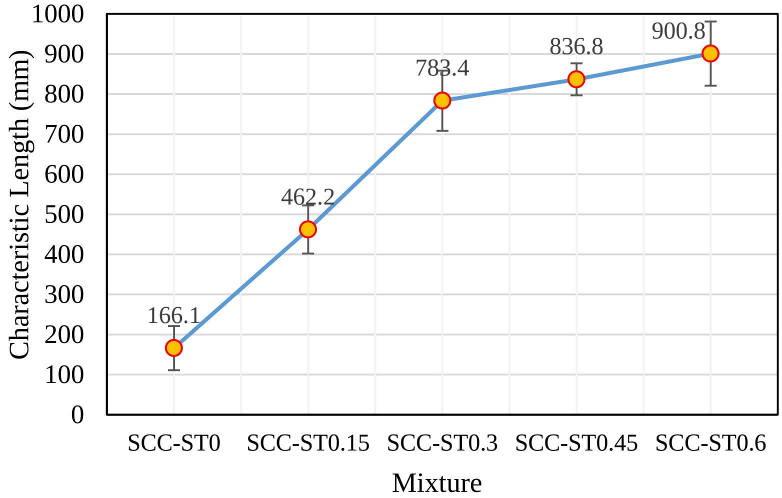

Figure 8. Characteristic length values versus steel fiber content in SCC samples

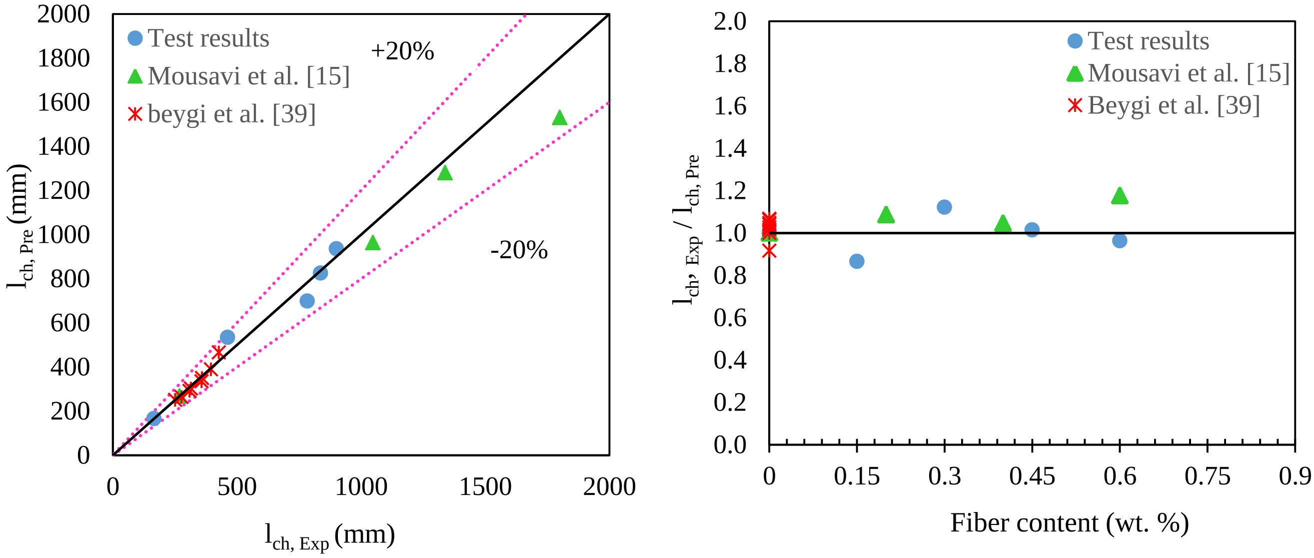

(a) **(b)**

Figure 9. (a) The results of developed characteristic length model of SCC compared with laboratory data of other researchers and present study; (b) the ratio of laboratory values to the predicted values of the characteristic length of SCC

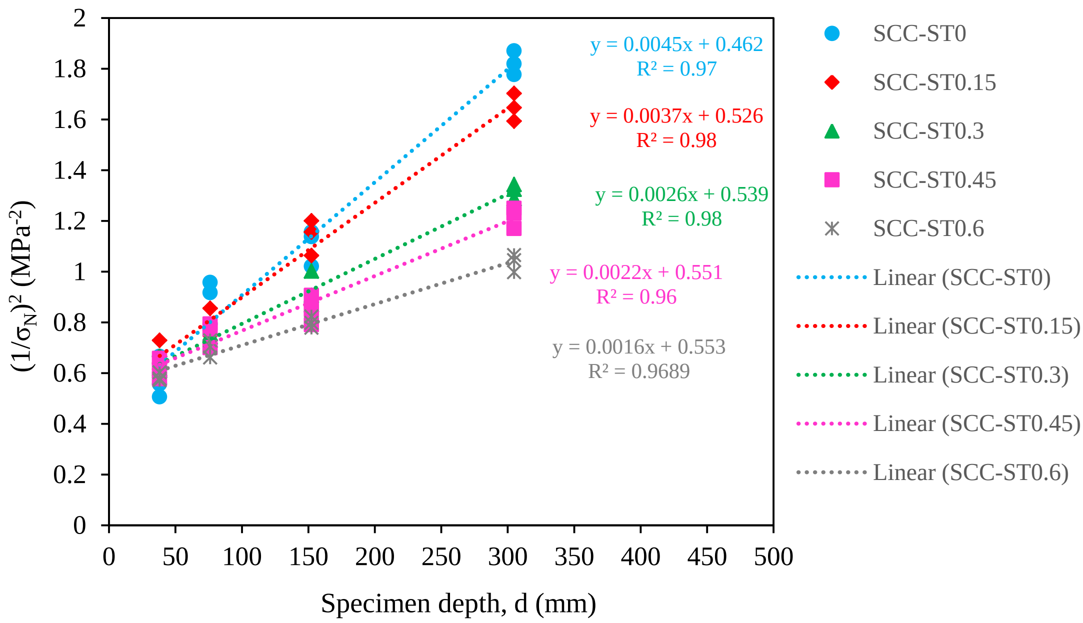

Figure 10. Fracture parameters of SCC samples incorporating steel fibers in SEM obtained using linear regression

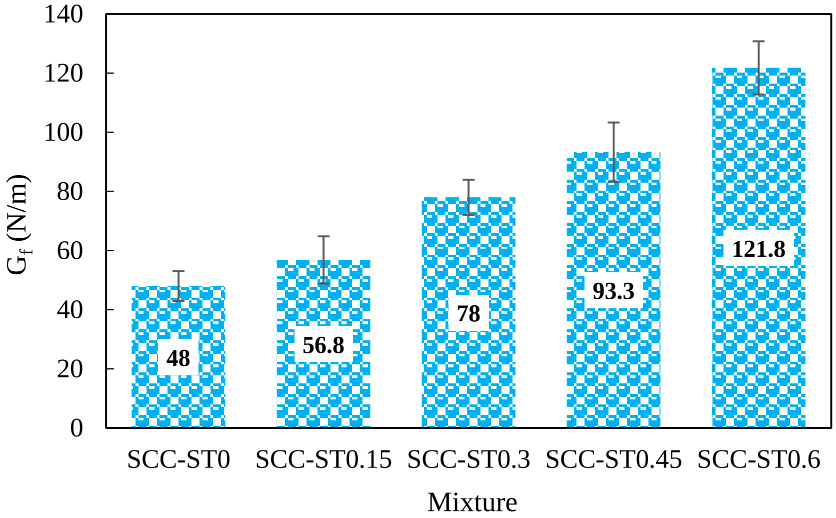

Figure 11. Initial fracture energy values against volume fraction of steel fibers

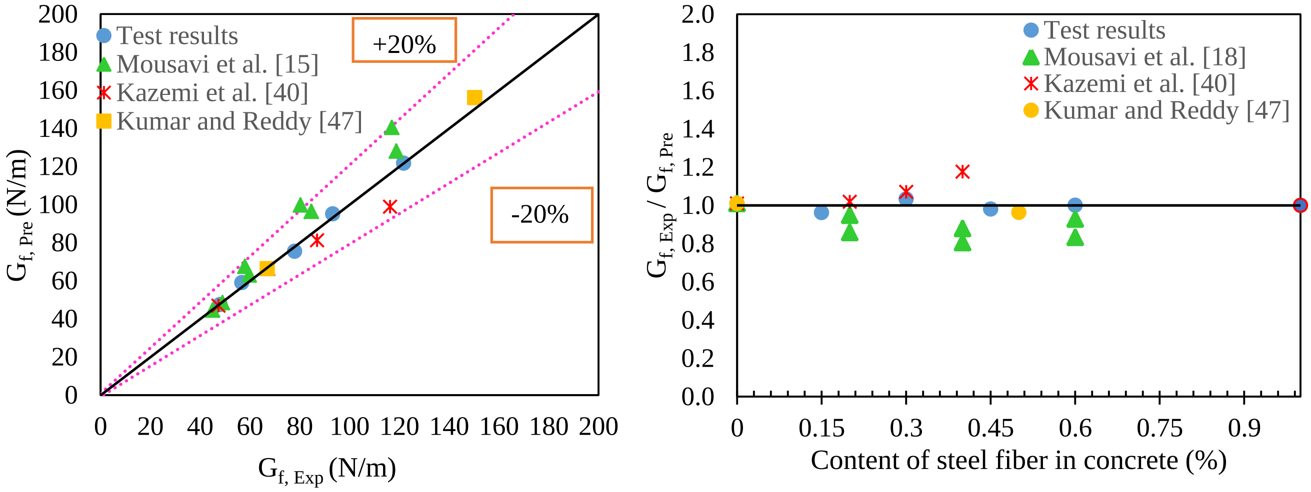

(a) **(b)**

Figure 12. (a) The proposed initial failure energy model compared with the laboratory results of other researchers and the present study; (b) the ratio of laboratory values to the predicted values of failure energy versus volumetric fraction of steel fibers

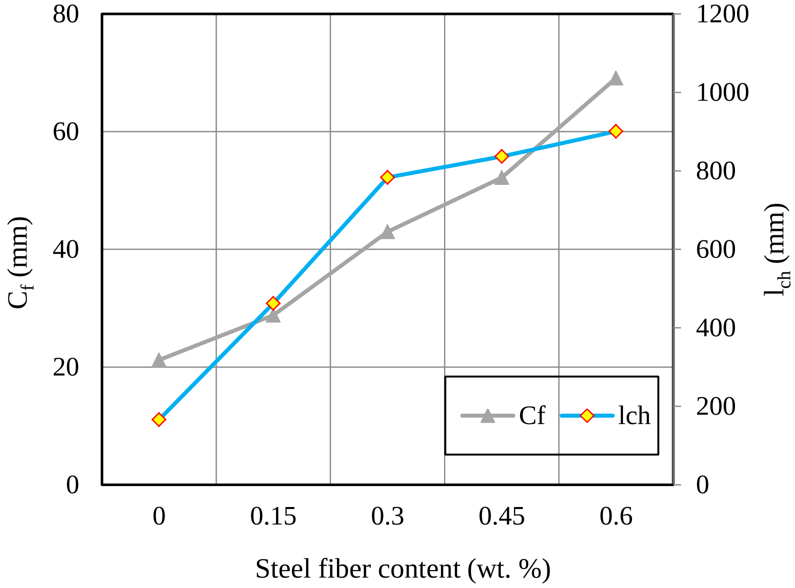

Figure 13. Variation of C_f with volume fraction of steel fibers for SCC samples

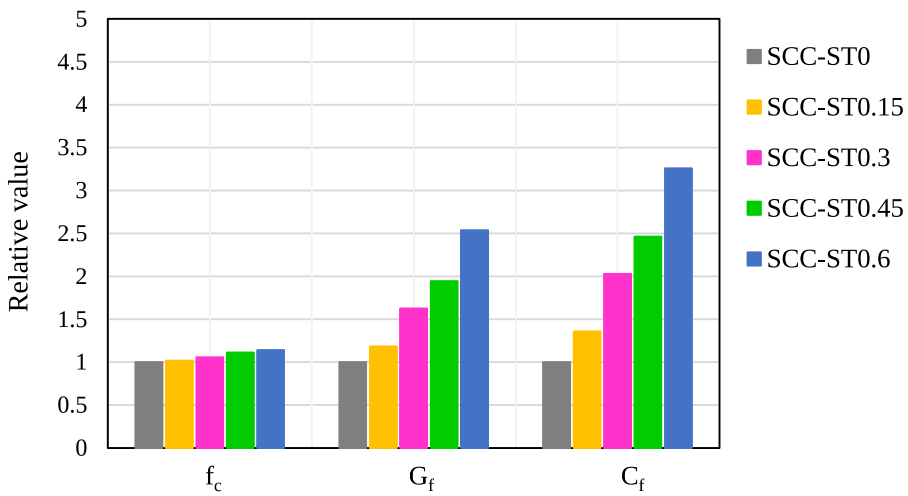

Figure 14. Concrete fracture parameters against volume fraction of fibers in SCC samples

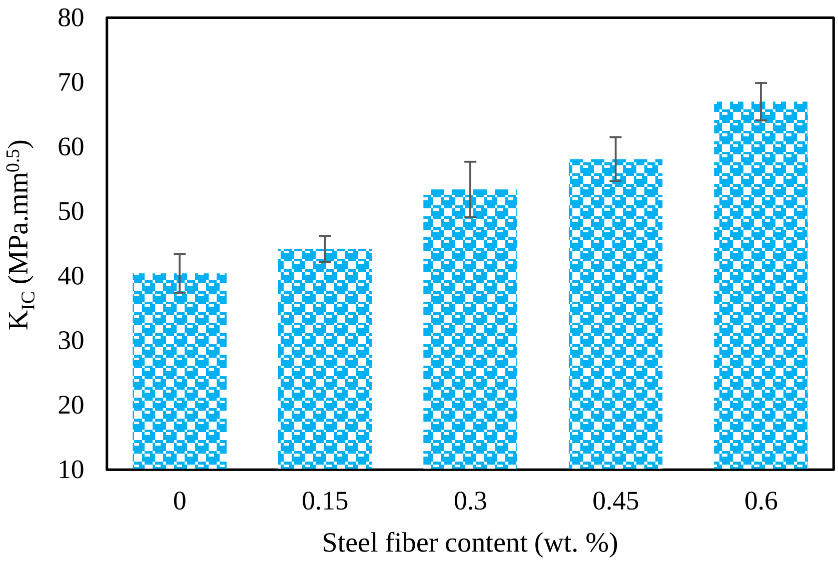

Figure 15. Fracture toughness for SCC samples against volumetric fraction of steel fibers

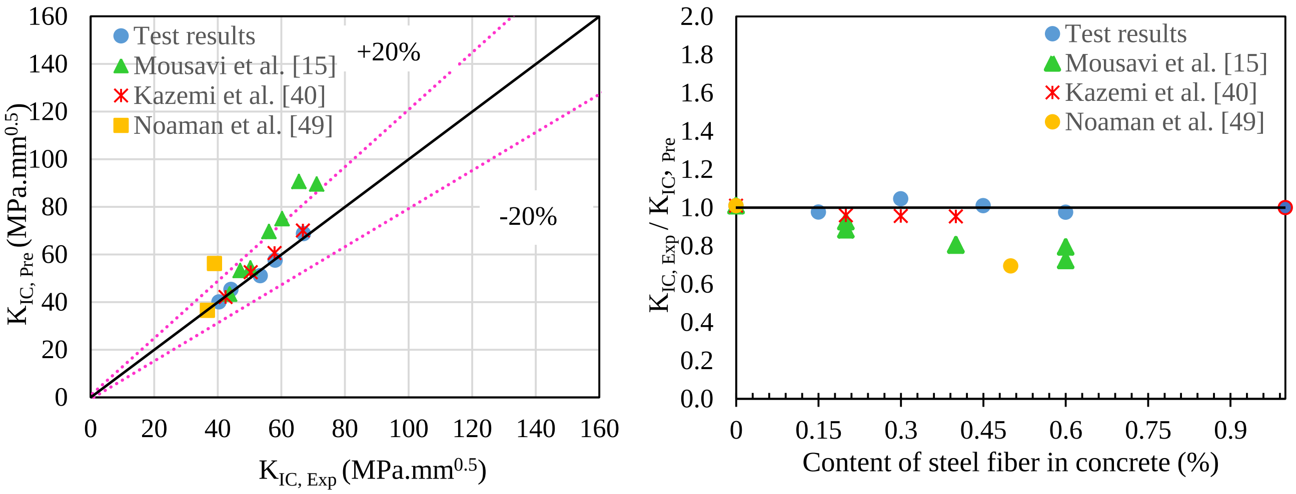

(a) **(b)**

Figure 16. (a) Results of developed fracture toughness model compared with laboratory data of present and other research works; (b) the ratio of laboratory values to predicted values versus the volume fraction of steel fibers

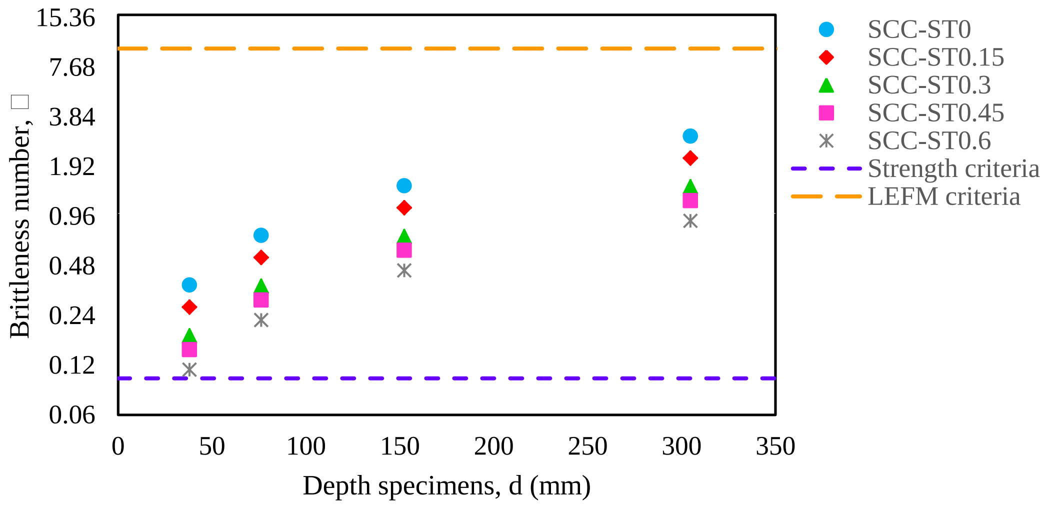

Figure 17. Variation of brittleness number (β) with the beam depth for SCC containing fibers

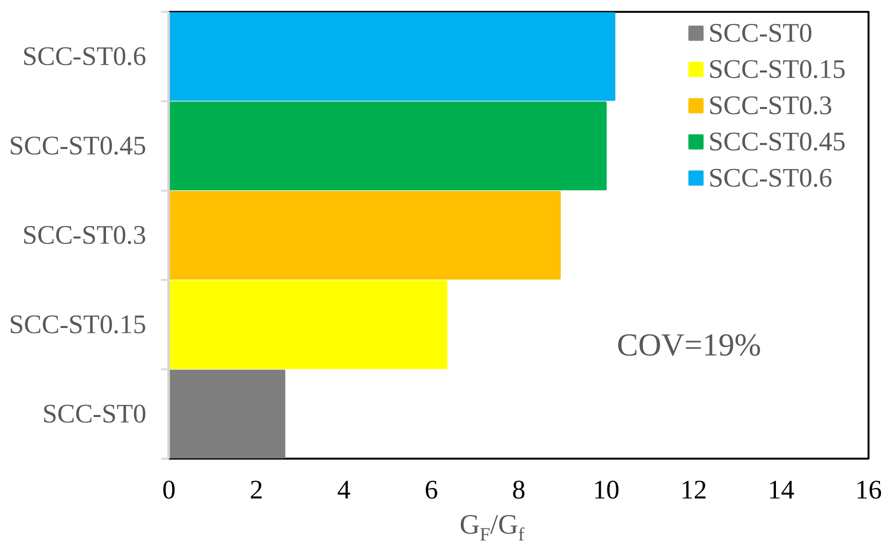

Figure 18. Total-to-initial fracture energy ratio for SCC incorporating different steel fiber contents

Table 1. Properties of steel fiber
Table 2. Mixture design proportions of SCC
Table 3. Specifications of fresh self-compacted concrete (SCC) as well as ranges proposed by EFNARC
Table 4. Dimensions and geometry of the SCC samples
Table 5. Details and mechanical features of SCC samples obtained based on WFM
Table 6. Maximum modified loads from the three-point flexural experiment of SEM samples
Table 7. Fracture parameters based on SEM

Table 1. Properties of steel fiber

Fiber type	**Shape**	**Length (mm)**	**Diameter (mm)**	**Aspect ratio** (l_f / d_f)	Tensile strength (MPa)	Elastic modulus (GPa)	Density (g/cm^3)
Steel	Hooked-end	35	0.8	43.75	1200	200	7.85

Note: l_f = length of fiber and d_f = diameter of fiber.

Table 2. Mixture design proportions of SCC

Mix No.	Mixture ID	V_f (%)	**W/C**	**Water**	**Cement**	**Limestone powder**	**Fine Aggregates**	**Coarse Aggregates**	**Superplasticizer (SP)**

							(kg/m^3)		
1	SCC-ST0	0	0.44	198	450	288	830	728	3.13
2	SCC-ST0.15	0.15	0.44	198	450	288	830	728	3.7
3	SCC-ST0.3	0.3	0.44	198	450	288	830	728	4.0
4	SCC-ST0.45	0.45	0.44	198	450	288	830	728	4.4
5	SCC-ST0.6	0.6	0.44	198	450	288	830	728	5.0

Table 3. Specifications of fresh self-compacted concrete (SCC) as well as ranges proposed by EFNARC

Fresh features	Ranges specified by EFNARC	SCC-ST0	SCC-ST0.15	SCC-ST0.3	SCC-ST0.45	SCC-ST0.6
Slump flow (mm)	650-800	765	760	758	730	715
Flow time (s)	2-5	3.1	3.3	3.5	4.1	4.7
V-funnel (s)	6-12	6.8	7.37	8.56	8.93	9.86
V-funnel at $T_{5minutes}$ (s)	Maximum 3s longer than V-funnel	7.25	8.87	10.29	10.72	11.02
L-Box (h_2/h_1)	0.8-1	0.96	0.93	0.90	0.88	0.85

Table 4. Dimensions and geometry of the SCC samples

Type of sample	Geometry	Dimension (mm)	Depth of notch (mm)
WFM notched beam	cuboid	100×`100×840	50

SEM notched beam	cuboid	38×38×101	8
		38×76×203	15
		38×152×406	30
		38×305×814	61
Compression sample	Cube	100×`100×100	-
Indirect tension sample	Cylinder	150×`300	-
Elastic modulus sample	Cylinder	150×`300	-

Table 5. Details and mechanical features of SCC samples obtained based on WFM

Mix ID	Steel fiber (V_f) (%)	f_c (MPa)	E (GPa)	f_t (MPa)	G_F (N/m)			Average G_F (N/m)	l_{ch} (mm)
					1	2	3		
SCC-ST0	0	51.40	34.10	5.10	123.5	126.2	130.4	126.7	166.1
SCC-ST0.15	0.15	52.30	34.40	5.18	369.2	360.4	351.9	360.5	462.2
SCC-ST0.3	0.3	54.30	36.50	5.70	692.8	690.2	708.9	697.3	783.4
SCC-ST0.45	0.45	57.20	36.20	6.35	926.7	937.2	932.4	932.1	836.8
SCC-ST0.6	0.6	58.60	36.90	7.13	1256.1	1248.7	1218.2	1241	900.8

Table 6. Maximum modified loads from the three-point flexural experiment of SEM samples

Mix ID	f_c (MPa)	a_0/d	d (mm)	Corrected peak load, P^0_n (N)		
				Beam 1	Beam 2	Beam 3
SCC-ST0	51.4	0.2	38.1	1779	1945	2040
			76.2	3259	3032	2967
			152.4	5746	5400	5443
			304.8	8711	8610	8492
SCC-ST0.15	52.3	0.2	38.1	1850	1780	1700
			76.2	3359	3400	3140
			152.4	5300	5630	5400

			304.8	8900	9050	9200
SCC-ST0.3	54.3	0.2	38.1	1859	1780	1850
			76.2	3340	3370	3400
			152.4	5800	6230	6100
			304.8	10090	10235	10020
SCC-ST0.45	57.2	0.2	38.1	1910	1790	1850
			76.2	3260	3470	3300
			152.4	6100	6530	6300
			304.8	10390	10735	10470
SCC-ST0.6	58.6	0.2	38.1	1909	1870	1920
			76.2	3460	3570	3400
			152.4	6400	6580	6500
			304.8	11250	11625	11360

Table 7. Fracture parameters based on SEM

Series	f_c **(MPa)**	**E (GPa)**	**a_0/d**	$g(\alpha_0)$	**G_f (N/m)**	**C_f (mm)**	**B (MPa)**	**d_0 (mm)**	**K_{IC} (MPa.mm$^{0.5}$)**	δ_c **(mm)**	ω_A	ω_c	**m**
SCC-ST0	51.40	34.10	0.2	7.28	48.0	21.2	1.47	103.7	40.4	0.017	0.058	0.097	0.11
SCC-ST0.15	52.30	34.40	0.2	7.28	56.8	28.8	1.38	141.0	44.2	0.022	0.049	0.062	0.082
SCC-ST0.3	54.30	36.50	0.2	7.28	78.0	43.0	1.36	210.5	53.4	0.031	0.041	0.035	0.055
SCC-ST0.45	57.20	36.20	0.2	7.28	93.3	52.2	1.35	255.5	58.1	0.037	0.068	0.047	0.081
SCC-ST0.6	58.60	36.90	0.2	7.28	121.8	69.1	1.34	338.1	67.0	0.048	0.057	0.030	0.056